# Synthesis and Characterization of Lignin Hydrogels for Potential Applications as Drug Eluting Antimicrobial Coatings for Medical Materials

Eneko Larrañeta,*,[†] Mikel Imízcoz,[†] Jie X. Toh,[†] Nicola J. Irwin,[†] Anastasia Ripolin,[†] Anastasia Perminova,[†] Juan Domínguez-Robles,[‡] Alejandro Rodríguez,[‡] and Ryan F. Donnelly[†]

[†]Belfast School of Pharmacy, Queen's University, 97 Lisburn Road, Belfast BT9 7BL, United Kingdom
[‡]Chemical Engineering Department, Universidad de Córdoba, Campus of Rabanales, Building Marie Curie, Córdoba 14071, Spain

Supporting Information

**ABSTRACT:** Lignin is the second most abundant biopolymer on the planet. It is a biocompatible, cheap, environmentally friendly and readily accessible material. It has been reported that these biomacromolecules have antimicrobial activities. Consequently, lignin (LIG) has the potential to be used for biomedical applications. In the present work, a simple method to prepare lignin-based hydrogels is described. The hydrogels were prepared by combining LIG with poly(ethylene glycol) and poly(methyl vinyl ether-co-maleic acid) through an esterification reaction. The synthesis took place in the solid state and can be accelerated significantly (24 vs 1 h) by the use of microwave (MW) radiation. The prepared hydrogels were characterized by evaluation of their swelling capacities and with the use of infrared spectroscopy/solid-state nuclear magnetic resonance. The prepared hydrogels showed LIG contents ranging between 40% and 24% and water uptake capabilities up to 500%. Furthermore, the hydrophobic nature of LIG facilitated loading of a model hydrophobic drug (curcumin). The hydrogels were capable of sustaining the delivery of this compound for up to 4 days. Finally, the materials demonstrated logarithmic reductions in adherence of *Staphylococcus aureus* and *Proteus mirabilis* of up to 5.0 relative to the commonly employed medical material poly(vinyl chloride) (PVC).

**KEYWORDS:** Lignin, Hydrogels, Drug delivery, Antimicrobial materials, Solid-state reactions, Microwave synthesis
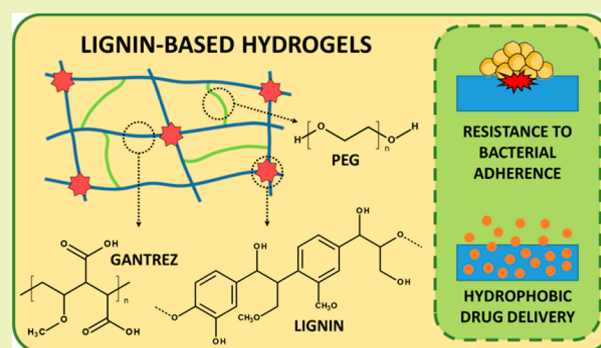
## INTRODUCTION

The global consumption of fossil fuels is steadily increasing due to industrial development and human population growth. Extensive efforts have been made to find green and sustainable alternatives for material production such as biorenewable polymers.[1] Ligno-cellulose materials have attracted significant attention due to their potential to reduce energy consumption and associated pollution by replacing conventional synthetic materials. This type of material is mainly formed by lignin (LIG), cellulose and hemicellulose.[1−6]

LIG is formed from a network of randomly cross-linked hydroxylated and methoxylated phenylpropane units. This molecule is present in the cell walls of cellulosic materials providing mechanical and chemical protection from external stresses. In addition to their mechanical properties, it has been reported that these biomacromolecules have antioxidant and antimicrobial activities.[7−10] Moreover, LIG is the second most abundant renewable biopolymer on the planet.[1,11] However, despite all these factors, LIG technologies remain significantly underdeveloped.[1,12] A minor fraction (less than 2%) of the approximate 70 million tons of LIG produced by the paper industry during the extraction of cellulose is reused for specialty

products.[1] The remainder is used as low grade burning fuel or discarded as waste.[1,13]

Extensive efforts have been made by the scientific community to develop new types of materials using LIG.[1] LIG has previously been used as a mechanical reinforcement for composites, an antioxidant, a UV protecting agent, an antimicrobial additive, a binder in lithium batteries, as material for water purification and as a biomedical material, among other applications.[1,11,14−20] With regards to biomedical applications, hydrogels represent one of the most highly employed materials within this field. Hydrogels are 3D-networks of polymeric chains cross-linked by physical or chemical interactions.[21,22] These materials are similar to biological tissue on account of their high water content and soft consistency.[21,22] LIG-based hydrogels could hold much promise as biomaterials due to the promising characteristics, including the antimicrobial activity, of this biomacromolecule.[7,11,23] Only a few examples have described the use of LIG to prepare hydrogels for biomedical

applications. The majority of these studies rely on complex synthetic procedures, involving toxic organic solvents or reagents,[1,24] which could ultimately limit applicability of the resulting hydrogels as biomaterials.

In the present work, we propose a facile way to prepare LIG-based hydrogels as potential medical material coatings. The hydrogels are prepared by combining LIG with poly(ethylene glycol) and poly(methyl vinyl ether-co-maleic acid) through an esterification reaction. The synthesis took place in the solid state and can be accelerated significantly by the use of microwave (MW) radiation. The hydrogels were characterized and their drug delivery and antimicrobial capabilities evaluated in vitro.

## ■ MATERIAL AND METHODS

**Materials.** Gantrez S-97 (GAN) (methylvinylether and maleic acid copolymer) (Mw = 1.2 × 10^{6} Da) was provided by Ashland (Tadworth, UK). Poly(ethylene glycol) (PEG) 10,000 and PEG 400 Da were obtained from Sigma-Aldrich (Dorset, UK). Glycerol (GLY) was obtained from VWR (Radnor, USA). LIG was obtained from Tokyo Chemical Industry UK Ltd. (Oxford, UK). CUR was purchased from Cambridge Bioscience (Cambridge, UK). Poly(vinyl chloride) (PVC) sheets (unplasticized, 0.2 mm thickness) were purchased from Goodfellow Ltd. (Cambridge, UK). *Staphylococcus aureus* ATCC 6538 and *Proteus mirabilis* ATCC 35508 (LGC Standards, Middlesex, UK) were maintained on cryopreservative beads (Protect Bacterial Preservation System, Technical Service Consultants Ltd., UK) in 10% glycerol at −80 °C. Strains were cultured by inoculation into MHB and incubated at 37 °C when required for the *in vitro* microbiological assessments.

**Lignin Characterization.** Lignin was analyzed with the purpose of establishing its physicochemical properties. Measurement of the major elements of this sample was carried out on a EuroEA3000 Elemental analyzer (EuroVector SpA, Italy) after drying the sample to be analyzed (30 mg) overnight at 105 °C.

Acid hydrolysis was performed to determine the Klason lignin and soluble lignin content.[25] Klason lignin content was determined by gravimetric yield and acid soluble lignin content was determined from the UV-absorption of the hydrolysate at 205 nm.[26] To determine the carbohydrate content, high-performance liquid chromatography (HPLC) analysis was preformed using a previously reported method.[27] Finally, the ash content of the lignin sample was determined gravimetrically by heating the sample to 800 °C and maintaining it at this temperature for 3–6 h until disappearance of the black carbon particles.

The Fourier transform infrared (FTIR) spectrum of the lignin was recorded using a Spectrum Two instrument (PerkinElmer, Waltham, MA, USA) equipped with an attenuated total reflectance (ATR) accessory. The spectrum was recorded as an average of 20 scans from 4000 to 450 cm^{−1} using a resolution of 4 cm^{−1}.

Solid-state ^{13}C nuclear magnetic resonance (NMR) spectra were recorded at 100.63 MHz using a Bruker Avance III HD spectrometer (Bruker, Leiderdorp, The Netherlands) and a 4 mm (rotor o.d.) magic-angle spinning probe. Spectra were obtained using cross-polarization with TOSS spinning sideband suppression, a 2 s recycle delay and 1 ms contact time at ambient probe temperature and at a sample spin-rate of 10 kHz. Spectral referencing was performed with respect to an external sample of neat tetramethylsilane (carried out by setting the high-frequency signal from adamantane to 38.5 ppm).

**Hydrogel Synthesis.** Ethanol/water (70% v/v) solutions containing LIG, GAN and PEG/GLY were prepared and 7.5 g of these solutions were cast in 5 cm × 5 cm molds. The ethanol/water solutions used in the present work contained 10% (w/w) of LIG, 5% (w/w) of GAN and 5% (w/w) of GLY or PEG. Solutions were allowed to dry over at least 48 h. The resulting films were cut into smaller pieces using a cork borer (diameter 1 cm) and subsequently placed inside an oven at 80 °C for 24 h. Subsequently, films were placed in an ethanol/water (70% v/v) solution for 1 week to remove

the unreacted reagents. This solution was replaced regularly. Hydrogels were also synthesized using a MW assisted procedure. This procedure is equivalent to the one previously described, but the thermal process (80 °C for 24 h) was replaced by a MW assisted process. Samples were placed inside a Panasonic NN-CF778S MW oven (Panasonic UK Ltd., Bracknell, UK) for 1 h at the maximum power setup (1000 W).

**Hydrogel Characterization.** Samples were analyzed using an FTIR Accutrac FT/IR-4100 Series (Jasco, Essex, UK) equipped with a MIRacle ATR accessory (64 scans and resolution of 4 cm^{−1}). Additionally, a Hitachi TM3030 scanning electron microscopy (SEM) instrument (Tokyo, Japan) was used to evaluate the morphology of the dry and freeze-dried hydrogels.

Solid-state ^{13}C NMR was used to estimate the composition of the hydrogels. The equipment and experimental conditions were as described in the Lignin Characterization section.

The swelling capabilities of the hydrogels were evaluated by weighing them ($m_0$), placing them in water and at regular intervals, the films were removed, dried with filter paper to eliminate excess surface water and weighed ($m_t$). The percentage swelling was calculated by eq 1.

$$\% \text{ Swelling} = \frac{m_t - m_o}{m_o} \times 100 \tag{1}$$

The average molecular weight between cross-links ($M_c$) was determined using the equilibrium swelling theory. $M_c$ was determined from swelling studies using the Flory and Rehner eq (eq 2).[28] All calculations were carried out using the data obtained after swelling the hydrogels in water over a 24 h time frame.

$$M_c = \frac{-d_p V_s \phi}{(\ln(1 - \phi) + \phi + \chi\phi^2)} \tag{2}$$

where $\phi$ is the volume fraction of the polymer in the swollen state (eq 3); $V_s$ is the molar volume of water (18 cm[3]/mol), and $\chi$ is the Flory−Huggins polymer−solvent interaction parameter (eq 4).[29]

$$\phi = \left[1 + \frac{d_p}{d_s}\left(\frac{m_a}{m_b}\right) - \frac{d_p}{d_s}\right]^{-1} \tag{3}$$

$$\chi = \frac{1}{2} + \frac{\phi}{3} \tag{4}$$

In order to calculate $\phi$ using eq 3, the following parameters were used: mass of hydrogel before swelling ($m_b$), mass of hydrogel after swelling ($m_a$), density of the hydrogel ($d_p$), and density of the solvent ($d_s$). The density of the hydrogel films was calculated using eq 5.

$$d_p = \frac{w}{S \times X} \tag{5}$$

where $X$ is the average thickness of the film, $S$ is the cross-sectional area, and $w$ represents the weight of the film.[30]

The cross-link density ($V_e$) was determined using eq 6,[30,31] where $N_A$ is Avogadro's number (6.023 × 10^{23} mol^{−1})

$$V_e = \frac{d_p \times N_A}{M_c} \tag{6}$$

**Curcumin Loading and Release.** All hydrogels were loaded with CUR by introducing a disc of the respective hydrogel into a glass vial containing 1 mL of CUR-acetone solution (20 mg/mL). After 24 h, the disc was dried at room temperature for a duration of ≥24 h. To determine total CUR loading, a piece of the disc was transferred into a vial with 20 mL of ethanol and after 24 h the released CUR was analyzed by UV−vis spectrometry (PowerWave XS Microplate Spectrophotometer, Bio-Tek, Winooski, USA) at a wavelength of 425 nm. To evaluate drug−polymer interactions, CUR loaded discs were cut in four fragments andanalyzed using a TA Instruments DSC Q100 differential scanning calorimeter (TA Instruments, New Castle,

**Table 1. Composition and Calculated Network Parameters for the LIG-Based Hydrogels**

| Hydrogel | Mw PEG | Weight ratio[a] | | Composition (%) (w/w)[a] | | | Network parameters | | | |
|---|---|---|---|---|---|---|---|---|---|---|
| | | LIG/GAN | LIG/PEG | LIG | GAN | PEG | $\phi$ | $M_c$ (Equi) (kDa) | $\chi$ | $V_e \times 10^{-19}$ |
| LIG14K | 14,000 | 1.5 | 1.3 | 41.1 | 27.4 | 31.6 | 0.15 | 70.0 | 0.55 | 0.96 |
| LIG10K | 10,000 | 1.4 | 1.1 | 38.1 | 27.2 | 34.7 | 0.17 | 40.9 | 0.56 | 1.59 |
| LIG400 | 400 | 0.9 | 0.5 | 24.3 | 27.0 | 48.6 | 0.21 | 18.4 | 0.57 | 3.59 |
| LIGGLY | −[b] | 0.5 | − | − | − | − | 0.17 | 46.5 | 0.56 | 1.54 |

[a]Calculated using solid-state $^{13}$C NMR measurements. [b]LIGGLY hydrogels contain GLY instead of PEG.

DE, USA). Samples were analyzed from 0 to 200 °C at a heating rate of 10 °C/min.

The release kinetics of CUR loaded discs were studied by introducing a weighed piece of disc into an Eppendorf containing 2 mL of a solution of 90% PBS and 10% Tween 80, to maintain sink conditions, with 0.1% ascorbic acid to prevent CUR degradation. The tubes were placed into an incubator (40 rpm and 37 °C). The concentration of CUR was evaluated at defined times using a UV−vis plate reader at a wavelength of 425 nm and after each measurement the medium was replaced with fresh media. For comparative purposes, the dissolution of pure CUR powder in the release media was evaluated. CUR powder (ca. 1 mg) was placed in a tube containing 16 mL of PBS (pH 7.3) with 10% of Tween 80 and 1 mg/mL of ascorbic acid.

**Analysis of Release Data.** The data obtained from the *in vitro* release experiments was fitted to the following mathematical models of drug release: the Korsmeyer-Peppas model (eq 11), the Higuchi model (eq 12) and the zero-order kinetic model (eq 13). In all cases, $M_t/M_\infty$ represents the fractional drug release at time $t$.

The Korsmeyer-Peppas model exponentially relates drug release with the elapsed time, $k_{KP}$ is the Korsmeyer-Peppas constant, and $n$ is the release exponent indicative of the drug release mechanism:[32,33]

$$\frac{M_t}{M_\infty} = k_{KP} \cdot t^n \tag{11}$$

The Higuchi model (eq 12) is used mainly for situations where Fickian diffusion governs the release process.[33] $k_H$ is the Higuchi constant.

$$\frac{M_t}{M_\infty} = k_H \cdot t^{0.5} \tag{12}$$

The zero-order kinetics eq (eq 13) is used when the system releases the same amount of drug per unit of time.[33] In this case, $k_{ZO}$ is the zero-order constant.

$$\frac{M_t}{M_\infty} = k_{ZO} \cdot t \tag{13}$$

**In Vitro Microbiological Assessment.** A GAN hydrogel containing no lignin (GANPEG) was prepared as one of the controls for the *in vitro* microbiological assessments, following the previously described procedure. For this purpose, an aqueous blend containing 20% (w/w) GAN and 7.5% (w/w) PEG was used. This hydrogel has been used and described extensively for drug delivery purposes.[30,34,35] Bacterial suspensions ($1 \times 10^6$ cfu mL$^{-1}$) of *P. mirabilis* and *S. aureus* were prepared as described in one of our previous works.[36] Hydrogel films and PVC controls (10 mm × 10 mm) were immersed in the bacterial suspensions (1 mL) within individual wells of a tissue culture plate. The materials had previously been soaking in deionized water for 0, 24 h, and 7 days. Samples were shaken at 100 rpm in an orbital incubator at 37 °C. Following 4 and 24 h incubation periods, samples were removed from the bacterial suspension, rinsed and sonicated in QSRS as described in our previous work.[36] Viable counts of the resulting QSRS were performed by the Miles and Misra serial dilution technique,[37] with plating onto low-swarm (LSW) agar (*P. mirabilis*) or Mueller-Hinton agar (*S. aureus*) to determine the number of adherent bacteria on each sample surface. Numbers of adherent bacteria after 4

and 24 h incubation are expressed as percentage values relative to PVC controls.

**Statistical Analysis.** All data were expressed as mean ± standard deviation. Data were compared using a One-Way Analysis of Variance (ANOVA), with Tukey's HSD posthoc test for more than two means. In all cases, $p < 0.05$ was the minimum value considered acceptable for rejection of the null hypothesis.

## RESULTS AND DISCUSSION

**Lignin Characterization.** LIG from a commercial source was selected for this work. Details of the major characteristics of the material, such as composition or origin, were, however, not provided. The complete LIG characterization can be found in the Supporting Information. Analysis of the LIG sample showed that ∼80% of the product was LIG (Table S1) and that there was a significant amount of inorganic particles (ca. 15%). Consequently, this reinforced the need to wash the hydrogels after synthesis to remove all impurities. Finally, the sample did not show any presence of cellulose contamination. The results obtained for the chemical composition and the FTIR and NMR analysis of the LIG samples (Figures S1 and S2) suggest that the lignin was isolated from wood using a pulping process containing sulfur delignifying agents and/or was precipitated using sulfuric acid.

**Lignin-Based Hydrogels Synthesis and Characterization.** LIG hydrogels were synthesized for potential biomedical applications by using GAN as a cross-linker. GAN/PEG hydrogels have been extensively studied for drug release applications.[34,38,39] These hydrogels are based on the esterification of the GAN acid groups with the OH groups present in PEG molecules.[34,38,39] LIG contains a large amount of alcohol groups and therefore represents an ideal candidate to be cross-linked with GAN. Additionally, GAN and LIG have been shown to be biocompatible and nontoxic.[40,41] Hydrogels were first prepared with GAN and LIG. However, the resulting films presented several limitations. The obtained films were not flat and were too brittle to handle in their dry state and therefore could not be used. It has been reported previously that GAN films are brittle in nature and they require a plasticizer to be used for drug delivery applications.[42] Additionally, after swelling, the materials disintegrated upon removal from the PBS solution as a result of their low cross-linking density and the swelling capacity of the hydrogels could therefore not be measured. The LIG employed presented a high molecular weight (ca. 60 kDa)[43,44] and, consequently, the resulting hydrogels presented an expanded structure that could accommodate large amounts of water. Consequently, a third component was added to provide a higher cross-linking degree and to act as a plasticizer of the films. PEG molecules seemed to be a good candidate for this purpose as they have been used previously as a GAN cross-linker.[34,38,39] Moreover, Singh et al. reported that PEG is a good plasticizer for GAN films.[42] Therefore, in the present study, PEG molecules with different
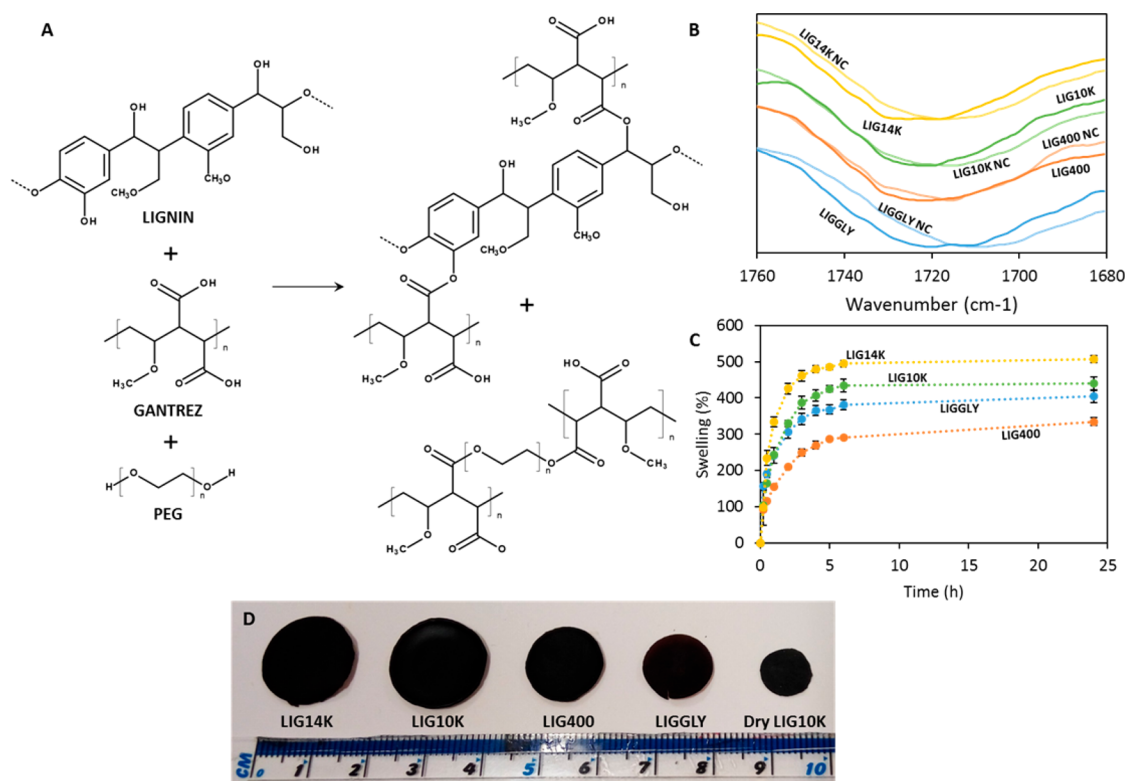
**Figure 1.** Chemical structure of LIG, GAN and PEG and proposed cross-linking reactions (A). FTIR spectra of the carbonyl region of of LIG/GAN/PEG hydrogels before (NC) and after the cross-linking process (B). Swelling kinetics of LIG-based hydrogels in PBS (C). Images of all swollen LIG-based hydrogels and the unhydrated LIG10K ($n = 3$) (D).

molecular weights were used as plasticizer/cross-linker to ascertain the effect of the PEG type on the properties of the final hydrogel (Table 1). In addition, GLY was used in order to evaluate the effect of a smaller molecule as a potential plasticizer/cross-linker (Table 1).

Figure 1 shows the chemical structures of LIG, GAN and PEG, and the proposed cross-linking reaction for the LIG/GAN/PEG hydrogels. It has previously been reported that GAN can be cross-linked with PEG via an esterification reaction.[30,34,38,39] Consequently, it was expected that a molecule with multiple OH groups such as LIG would be facilely added to the structure (Figure 1). A similar behavior was expected when combining GAN, LIG and GLY because the GLY molecule contains three OH groups.

The esterification reaction takes place in the solid phase. Therefore, we can hypothesize that before the cross-linking reaction some of the OH groups present in PEG/LIG are aligned with the COOH groups present in GAN chains, forming hydrogen bonds, as previously proposed by Singh et al.[42] During the cross-linking process, the supplied thermal energy allows the formation of ester bonds between the previously aligned COOH and OH groups.

To ascertain the cross-linking chemical reaction, FTIR spectroscopy was used. Representative spectra of the pure compounds and non-cross-linked and cross-linked hydrogels can be found in the Supporting Information (Figure S3). The main changes are within the carbonyl region. GAN carboxylic acids react with alcohol groups in LIG and PEG to form ester bonds. Figure 1B shows the FTIR spectra of the carbonyl region for the hydrogels before and after the cross-linking reaction. It is noticeable that the carbonyl peak shows a displacement to higher wavenumbers after the cross-linking

process. The infrared carbonyl peaks for the carboxylic acids and esters are overlapping and the peak shift suggests the presence of a new ester peak that overlaps with the previous acid peak.[36,45]

To determine the amount of GAN, PEG and LIG in the hydrogels, solid-state $^{13}C$ NMR was used. Table 1 shows the composition of the hydrogels measured using solid-state 13C-NMR (see Supporting Information Figure S4). The composition of the LIGGLY hydrogel could not be estimated due to the low intensity and overlap of the peak assigned to GLY at 77−66 ppm with peaks from GAN and LIG. On the other hand, the obtained results for the remaining hydrogels showed that the amount of GAN remained almost unaltered for all hydrogels at approximately 27% (w/w). LIG14K and LIG10K showed similar compositions, with a LIG percentage of ∼40% (w/w) and a PEG concentration of ∼32% (w/w). LIG400 showed a lower LIG concentration, ∼25% (w/w), and a higher PEG concentration. As described before, the composition of LIGGLY hydrogels could not be fully analyzed as the GLY peak is so small that it is overlapping with the LIG peaks. Consequently, the GLY concentration could not be properly calculated but we can assume that it is significantly lower than the PEG composition in the previous hydrogels. Moreover, it can be seen that the 13C-NMR spectrum of LIGGLY showed smaller LIG associated peaks (158−100 ppm) than the rest of the hydrogels. By comparing the peaks at 185−165 ppm and 158−100 ppm it can be estimated that LIGGLY presented the lowest LIG/GAN weight ratio (0.5).

The results showed that the GAN concentration remained almost constant and the LIG concentration decreased while the PEG concentration increased. This suggests that the molecular weight of the second cross-linker significantly influenced the

ability of LIG to bind to the GAN structure. It can be hypothesized that when GAN was cross-linked with the higher molecular weight PEG, the network had more space to accommodate LIG molecules within the structure. On the other hand, when smaller cross-linkers were used, the network presented a more compact structure that prevented ready accommodation of LIG within the structure. It is important to note that when using GLY as a cross-linker the effect is slightly different. We obtained hydrogels with a lower LIG content and a low GLY content that could not be properly determined. This suggest that LIG prevents the reaction of GAN with GLY. Therefore, the resulting hydrogels are formed mainly by GAN and LIG.

In order to gain more understanding about the hydrogel structure and the corresponding behavior when placed in contact with an aqueous environment, the swelling kinetics of the materials in PBS were studied. Figure 1C shows the swelling curves as a function of time for all synthesized hydrogels. It can be seen that all hydrogels showed similar swelling profiles, reaching the maximum water uptake after approximately 5 h. All hydrogels presented different maximum water uptakes ($p < 0.05$). LIG14K showed the highest degree of swelling, followed by LIG10K. This was expected since the composition of both hydrogels was similar but LIG14K had a longer cross-linker (PEG 14,000 vs PEG 10,000). The only two hydrogels that showed no significant difference in their maximum water uptakes were LIGGLY and LIG10K ($p = 0.215$). Interestingly, LIG400 showed a lower swelling capacity than LIGGLY. LIG400 showed a high amount of PEG 400 in the hydrogel (Table 1) suggesting that this linear polymer was the main cross-linker limiting incorporation of LIG in the structure. Additionally, Table 1 showed that these hydrogels presented the lowest LIG/GAN ratios. As explained previously, the NMR analysis suggested that LIGGLY hydrogels were formed mainly from GAN and LIG. These hydrogels contained a small amount of GLY and consequently the cross-linking of GAN with LIG molecules will lead to a more loosely cross-linked structure and higher swelling degrees than LIG400 that contains LIG and PEG400 as cross-linkers. This hypothesis would explain why LIGGLY did not present the lowest degree of swelling. Moreover, Figure 1D shows representative images of the swollen hydrogels. For comparative purposes, a sample of unhydrated LIG10K was included in the images. Interestingly, LIGGLY hydrogels appeared smaller in size than the LIG400 hydrogels despite having a higher swelling capacity. As can be seen in Table 1, LIGGLY presented the lowest LIG/GAN ratio. A high amount of the initial LIG did not react with GAN chains and, consequently, was washed away after synthesis. Therefore, LIGGLY hydrogels are significantly smaller after washing. GAN-based hydrogels have previously been prepared using different types of cross-linkers such as poly(vinyl alcohol), GLY, PEG or poloxamers.[46−51] However, the majority of these hydrogels showed higher swelling degrees as they only used one cross-linker.

Table 1 shows the calculated network parameters for all synthesized hydrogels. As expected, the average molecular weight between cross-links increased with the swelling capacity of the hydrogels. The volume fraction of polymer in the swollen state ($\phi$) is described as a ratio of the polymer volume to the swollen gel volume (eq 3).[30] As can be seen in Table 1, the hydrogels with higher swelling capacity showed higher $\phi$ values. The higher the value of $\chi$, the weaker was the interaction between the polymer and water. Therefore, increasing the

cross-linking degree increased the interaction between the polymeric system and water. Finally, $V_e$ represents the number of elastically effective chains, totally induced in a perfect network, per unit volume.[30,31] Consequently, hydrogels with higher cross-linking densities presented higher values of $V_e$. The calculated $V_e$ values were consistent with the results obtained in the swelling studies.

Figure 2 shows SEM images of the hydrogels after swelling/freeze-drying. The SEM images of the hydrogels before swelling
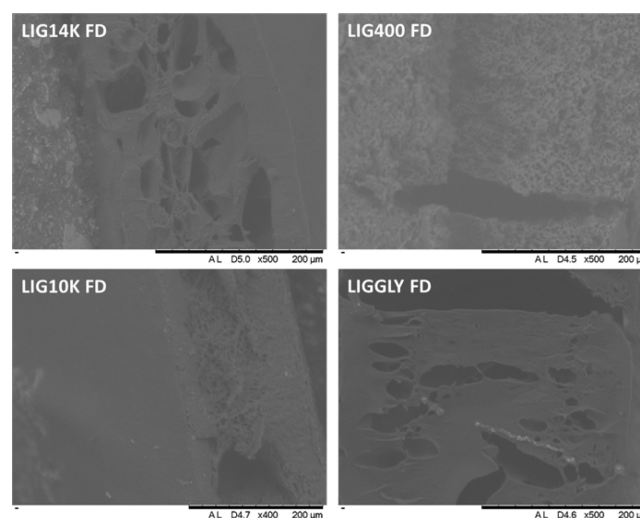


**Figure 2.** SEM images of freeze-dried (FD) hydrogels.

can be seen in the Supporting Information (Figure S5). It can be seen that all the dry hydrogels showed a certain degree of porosity that can be attributed to LIG. The only exception was LIGGLY, which showed a highly compact structure. From analysis of the NMR results it was obvious that these hydrogels were mainly formed by GAN and LIG, presenting a lower LIG/GAN ratio (0.5). Consequently, the lower LIG content would explain the compact structure. Additionally, the freeze-dried hydrogels showed bigger pores (see Supporting Information Figure S5). The pore sizes could be correlated with the maximum water uptake. LIG14K, LIG10K and LIGGLY showed larger holes and pores in their structure after removal of the water, while LIG400 showed a more uniform and smaller pore size distribution. This was a direct consequence of its lower water uptake.

All results shown in this section support the use of the process developed herein for the preparation of LIG-based hydrogels. The synthetic process does not require the use of any toxic solvents or reagents. The solvent employed was an ethanol/water mixture, and it has been previously reported that methanol/water or ethanol/water mixtures are environmentally favorable compared to other types of organic solvents such as pure alcohol or propanol/water mixtures.[52] Furthermore, the cross-linking reaction is an esterification process and the main byproduct of these reactions is water. Consequently, it can be established that the process is a green process as the used reagents did not present any danger or toxicity for the environment and no toxic side-products were generated.

**Curcumin Loading and Release from the Lignin-Based Hydrogels.** Several authors have reported the inclusion of hydrophobic moieties within hydrogel structures as a mechanism of improving hydrophobic drug loading.[53] Consequently, LIG-based hydrogels have potential to be used as

hydrophobic drug delivery systems. CUR was selected as a model hydrophobic compound to evaluate the capability of LIG-containing hydrogels to load and release hydrophobic drugs. Figure 3A shows the obtained CUR loading for all the
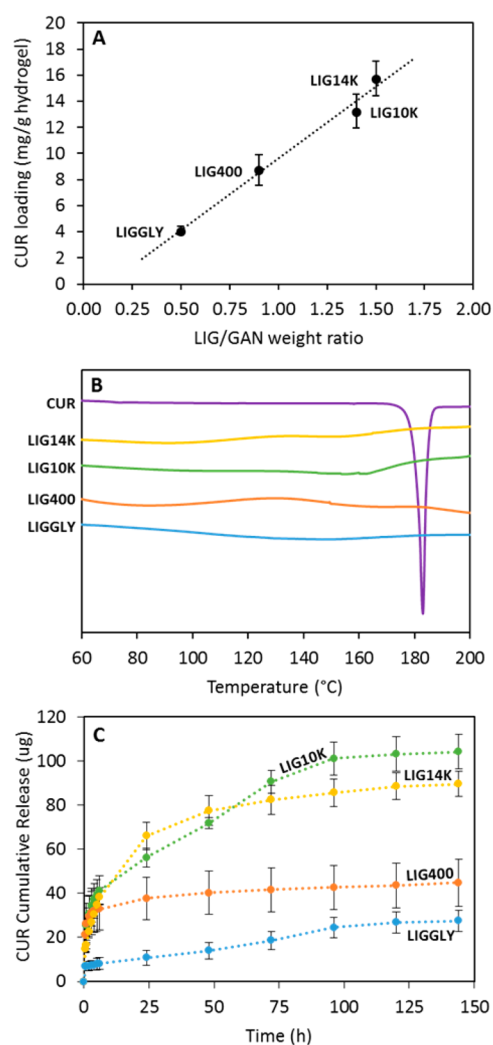


**Figure 3.** Correlation between the CUR loading and the LIG/GAN weight ratio in the hydrogels ($n = 3$) (A). DSC curves for CUR and CUR loaded hydrogels (B). For all thermograms: Exo Up. CUR cumulative release from all the hydrogels (C). ($n = 3$).

LIG-containing hydrogels. It can be seen that the hydrogels with higher LIG content presented higher CUR loading and the loading can be correlated with the LIG/GAN weight ratio of the hydrogels. LIG is a molecule rich in aromatic rings and CUR contains two aromatic rings. Consequently, the interaction between aromatic rings could explain this trend. The interaction between CUR molecules and other aromatic ring-containing molecules has been extensively described in the literature.[54] All the hydrogels presented different degrees of CUR loading ($p < 0.05$). However, there were no significant differences between LIG14K and LIG10K loadings ($p = 0.091$). This hypothesis can be confirmed through DSC measurements (Figure 3B). The CUR DSC curve showed a sharp endothermic melting point at around 180 °C. This peak cannot be observed in the hydrogels loaded with CUR suggesting that cargo molecules are interacting with the hydrogel structure and consequently they are not forming

crystals. In the literature, similar results can be found for other types of CUR supramolecular complexes such as CUR/cyclodextrin complexes.[55]

Figure 3C and Figure S6 (Supporting Information) show CUR cumulative release from all synthesized hydrogels. It can be seen that LIG14K and LIG10K released the largest amount of CUR, followed by LIG400 and then LIGGLY. This was consistent with the loading results. Moreover, it can be seen that LIG400 did not show a sustained release since the hydrogels released all their CUR cargo within a few hours. The other hydrogels showed CUR release over several days, and up to 4 days for LIG10K and LIGGLY. The latter showed promising capabilities for sustaining the release, however, it is not an ideal candidate due to the poor CUR loading. The optimal hydrogels in terms of CUR loading and release were LIG14K and LIG10K. LIG10K showed a linear release profile after an initial burst release of the cargo. On the other hand, LIG14K hydrogels did not show this biphasic pattern in their release profiles. Both hydrogels contained similar LIG concentrations. Consequently, it seems that as LIG10K showed a lower water uptake capacity (Figure 1C) it presented a more compact structure and a slower diffusion of CUR from the hydrogel matrix. The solubility of CUR was not the main factor behind the sustained release of CUR from the hydrogels as the dissolution of equivalent amounts of pure CUR powder was complete within 3−4 h (data not shown).

In order to ascertain the release mechanism of CUR from the hydrogels, different mathematical models were used. Table S3 (Supporting Information) shows calculated parameters obtained after fitting the release data to the equations described in the material and methods section. The results showed that the only hydrogel showing a diffusion-based release mechanism was LIG14K, with $n$ value close to 0.45 for the Korsmeyer-Peppas model and good fitting to the Higuchi model (Fickian diffusion model). On the other hand, LIGGLY and LIG10K presented linear release after the initial burst release. Their lineal section showed good fit to the zero-order model (see Supporting Information Table S3). This can be explained by the similar swelling profile of both hydrogels. However, LIGGLY presented poor CUR loading capabilities. Overall, after evaluating the composition and behavior of the hydrogels and by evaluating the CUR release kinetics, we can conclude that LIG10K showed the most promising capabilities for biomedical applications (high lignin content, high CUR loading while providing sustained release). Consequently, LIG10K was used in the following studies to evaluate the antimicrobial properties of LIG-based hydrogels.

**In Vitro Microbiological Assessment.** Nosocomial infections primarily result from bacterial attachment to surfaces, for example of implanted medical devices, and resulting biofilm formation.[56] These infections demonstrate significant resistance to antibacterial treatment, resulting in extended hospital stays, increased healthcare costs, patient morbidity and potential mortality.[57] Consequently, antimicrobial materials/coatings have attracted the attention of researchers during recent years.[58,59] Due to the antimicrobial properties of LIG, the LIG10K hydrogels were evaluated as potential antimicrobial coatings for medical devices. The LIG10K hydrogel and a control hydrogel (GANPEG) (without LIG) were herein tested for their in vitro resistance to adherence of the Gram-positive pathogen, *Staphylococcus aureus* (Figure 4ia), a common causative agent of nosocomial bloodstream and medical device-associated infections[60] and the Gram-negative urinary
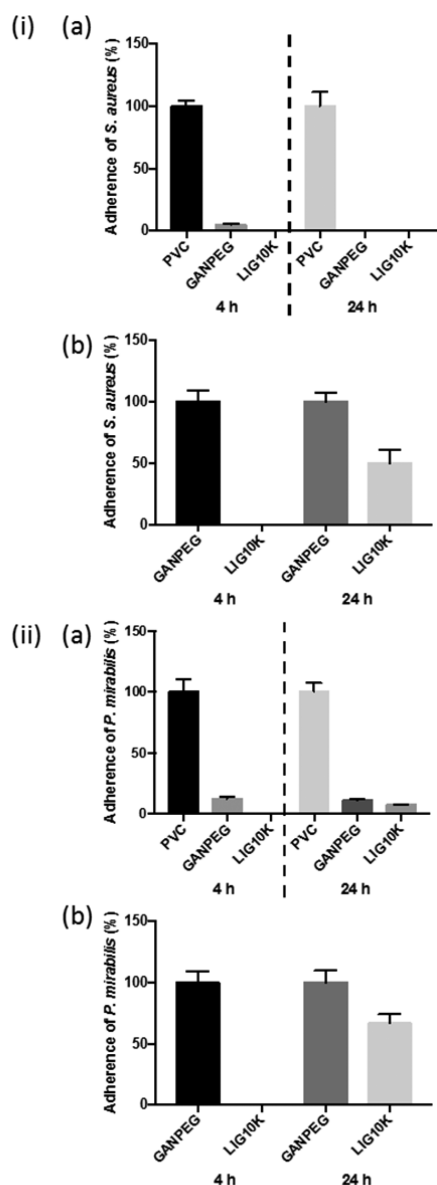
**Figure 4.** Adherence (%) of (i) *S. aureus* and (ii) *P. mirabilis* to surfaces of LIG10K presoaked in deionized water for 7 days relative to (a) PVC and (b) GANPEG controls after 4 and 24 h incubation at 37 °C. Columns and error bars represent means ± standard deviations ($n \geq 5$).

pathogen, *Proteus mirabilis* (Figure 4iia), a leading cause of catheter-associated urinary tract infections[61] relative to a common medical device material, PVC.[62]

Figures 4ia and 4iia show that samples of GANPEG and LIG10K hydrogels soaked in deionized water for 7 days demonstrated significantly greater resistance to adherence of both pathogens relative to PVC controls after challenge periods up to 24 h. Figures S7 and S8 (see Supporting Information) show similar results for the unwashed and 24h soaked samples. The observed durability and retention of antibacterial properties after rinsing is important with regards to clinical application of the lignin-containing materials as medical device coating technologies, and the associated need for prevention of infection throughout the period of device implantation.[63] The antibacterial activity of GAN-based hydrogels has previously been reported.[64,65] To determine the antibacterial effect of the

LIG component, bacterial adherence to the seven-day soaked LIG10K hydrogels was expressed relative to the GANPEG materials, and the significantly greater resistance to adherence of *S. aureus* and *P. mirabilis* of the LIG-containing hydrogels can be seen in Figures 4ib and 4iib.

While this is the first report of the antibacterial properties of GAN-LIG hydrogels, LIG has previously demonstrated promising antimicrobial activities toward cultures of Gram-positive bacteria and yeast.[15,66] With respect to the activity of LIG toward Gram-negative bacteria, mixed findings have been reported. No efficacy of LIG samples toward Gram-negative bacteria was reported in studies by Nada et al. and Dong et al., whereas Yang et al. have recently demonstrated promising capacity of LIG-nanoparticle-containing nanocomposite films based on poly(vinyl alcohol) and chitosan in inhibiting the growth of two Gram-negative pathogens.[15,67,68]

The encouraging resistance of the LIG-based hydrogels to adherence of the two pathogens observed herein offers promise for exciting new applications of this biomacromolecule in biomedical fields, where nonfouling materials and nonresistance-promoting antimicrobial strategies are urgently required. Moreover, due to the capability of sustaining drug release over several days, these materials can be loaded with antimicrobial compounds or other drugs to enhance their antimicrobial capabilities and deliver drugs to improve therapeutic outcomes.

**3.5. Microwave-Assisted Cross-Linking of LIG-Based Hydrogels.** As previously mentioned, the developed process can be considered a green process due to the lack of toxicity of any of the solvents or byproducts. Besides, the process is simple and can be performed in the solid state after combining the reagents. However, the cross-linking time is long and requires temperatures of 80 °C over 24h. This is acceptable at the laboratory scale but would be a limiting factor for industrial production. In order to obtain LIG-based hydrogels by a more efficient cross-linking process we explored the use of MW radiation.

The cross-linking process was ascertained with FTIR spectroscopy (Figure 5A). It can be seen that the GAN carbonyl peaks presented a shift due to the esterification reaction.[45] The peaks displayed higher shifts after the MW treatment than after the conventional oven treatment (Figure 1B). This suggests that the cross-linking process was more efficient since the hydrogels presented a higher degree of esterification after the 1 h treatment than after 24 h with the conventional process.

The water uptake of the obtained hydrogels was evaluated (Figure 5B). LIGGLY hydrogels obtained from the MW assisted procedure were brittle and the swelling study could not be completed due to disintegration of the samples during the swelling process. It can be seen that the swelling profiles remained similar but the degree of swelling was significantly lower than for the hydrogels prepared using the conventional process. In order to compare the degree of swelling of the cross-linked materials prepared using both processes, Figure 5C shows the maximum swelling of all the formulations. It is obvious from this figure that the MW process yields hydrogels with higher cross-linking degrees due to the lower extent of swelling than for the oven cross-linked hydrogels ($p < 0.05$).

The mechanism behind the MW-assisted cross-linking of the hydrogels is still unknown. We mentioned before that the OH and COOH groups should be aligned in the films before the cross-linking reaction. We hypothesize that the MW radiation provides a more efficient way of providing the energy required
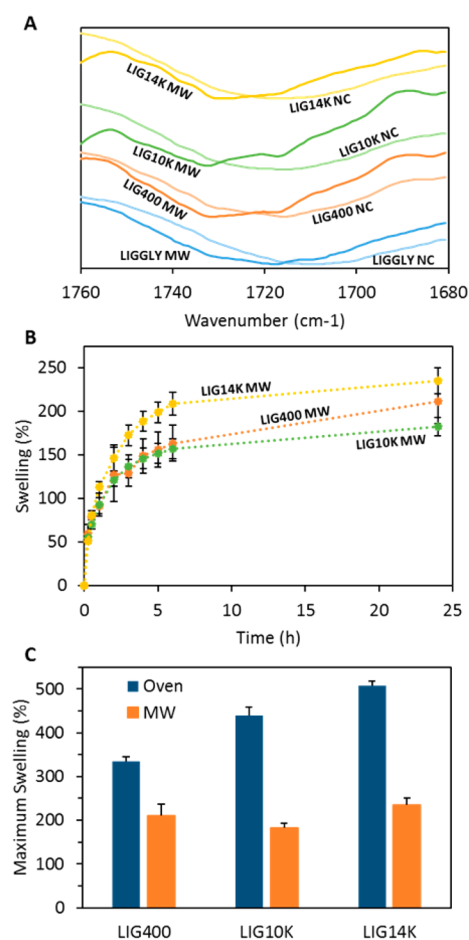
**Figure 5.** Carbonyl region of LIG/GAN/PEG hydrogels before (NC) and after the MW-assisted cross-linking process (A). Swelling kinetics in PBS of LIG-based hydrogels cross-linked using the MW-assisted process (B). Maximum swelling in PBS of LIG-based hydrogels cross-linked in the oven and in the microwave (C). ($n$ = 3).

for the esterification reaction. Conventional ovens heat the material from the outside. On the other hand, microwave radiation penetrates into the materials providing volumetric heating,[69] allowing a more efficient cross-linking reaction. Finally, MW heating is more efficient and likely to have higher temperatures than during the conventional process.

More experiments should be done to optimize MW-assisted cross-linking of LIG hydrogels. However, the promising results shown here suggest that the cross-linking process can be improved significantly. The MW process is shorter, more sustainable as it requires less energy than the thermal process[34] and, overall, it will lead to the production of lower cost materials.

## CONCLUSIONS

The present work describes a simple, green procedure to prepare LIG-based hydrogels. The process does not require the use of toxic solvents and one of the main components of the hydrogel is a renewable material. LIG hydrogels were successfully obtained after combination of the biomolecule with GAN, a polyacid and PEG through an esterification reaction. It was demonstrated that the molecular weight of the PEG influenced hydrogel properties, including the final LIG content and water uptake capacity. The prepared hydrogels showed LIG contents ranging between 40% and 24% and water

uptake capabilities up to 500%. The highest LIG contents and swelling capacities were obtained when PEGs with higher molecular weights of 14,000 and 10,000 were used. The prepared hydrogels were able to be loaded with hydrophobic compounds and to sustain the release for up to 4 days. Hydrogels obtained by using PEG with a molecular weight of 10,000 showed the best properties in terms of drug loading and release. Additionally, the antimicrobial properties of LIG-based hydrogel materials cross-linked using PEG 10,000 were evaluated using two common pathogens responsible for medical device-associated infections, *S. aureus* and *P. mirabilis*. The results of these studies demonstrated that LIG-based hydrogels showed significant resistance to bacterial adherence when compared to PVC and similar hydrogels that do not contain LIG. Consequently, LIG-based hydrogels present promising properties as medical material coatings based on their resistance to infection and ability to release drugs over several days. Finally, we demonstrated that the hydrogel preparation can be accelerated by using MW radiation. In this way, the cross-linking time was reduced from 24 to 1 h by using the MW-assisted process, thereby lowering the energy consumption. This was a proof of concept and more work is needed to optimize the MW cross-linking step; however, these findings suggest that MW treatment can be used as an alternative way to obtain LIG-based hydrogels in an easier, lower cost and greener way.

## ASSOCIATED CONTENT

**⑤ Supporting Information**

The Supporting Information is available free of charge on the ACS Publications website at DOI: 10.1021/acssusche-meng.8b01371.

Pure lignin/hydrogel FTIR spectra, solid-state $^{13}$C NMR and SEM images, results obtained for curcumin release mathematical modeling and *in vitro* microbiological assessment results (PDF)

## AUTHOR INFORMATION

**Corresponding Author**

*Dr. Eneko Larrañeta. Tel: +44 (0)28 9097 2360. Email: e.larraneta@qub.ac.uk.

**ORCID** ⓘ

Eneko Larrañeta: 0000-0003-3710-0438
Alejandro Rodríguez: 0000-0001-8196-5848

**Author Contributions**

The first three authors contributed equally.

**Notes**

The authors declare no competing financial interest.

## ACKNOWLEDGMENTS

## REFERENCES

(1) Kai, D.; Tan, M. J.; Chee, P. L.; Chua, Y. K.; Yap, Y. L.; Loh, X. J. Towards lignin-based functional materials in a sustainable world. *Green Chem.* **2016**, *18*, 1175−1200.

(2) Palm, M.; Zacchi, G. Separation of hemicellulosic oligomers from steam-treated spruce wood using gel filtration. *Sep. Purif. Technol.* **2004**, *36*, 191−201.

(3) Laurichesse, S.; Avérous, L. Chemical modification of lignins: Towards biobased polymers. *Prog. Polym. Sci.* **2014**, *39*, 1266−1290.

(4) Doherty, W. O. S.; Mousavioun, P.; Fellows, C. M. Value-adding to cellulosic ethanol: Lignin polymers. *Ind. Crops Prod.* **2011**, *33*, 259−276.

(5) Thakur, V. K.; Thakur, M. K.; Gupta, R. K. Graft copolymers from cellulose: Synthesis, characterization and evaluation. *Carbohydr. Polym.* **2013**, *97*, 18−25.

(6) Figueiredo, P.; Lintinen, K.; Hirvonen, J. T.; Kostiainen, M. A.; Santos, H. A. Properties and chemical modifications of lignin: Towards lignin-based nanomaterials for biomedical applications. *Prog. Mater. Sci.* **2018**, *93*, 233−269.

(7) Thakur, V. K.; Thakur, M. K. Recent advances in green hydrogels from lignin: a review. *Int. J. Biol. Macromol.* **2015**, *72*, 834−847.

(8) Domínguez-Robles, J.; Espinosa, E.; Savy, D.; Rosal, A.; Rodríguez, A. Biorefinery Process Combining Specel® Process and Selective Lignin Precipitation using Mineral Acids. *BioResources* **2016**, *11*, 7061−7077.

(9) Sánchez, R.; Espinosa, E.; Domínguez-Robles, J.; Loaiza, J. M.; Rodríguez, A. Isolation and characterization of lignocellulose nano-fibers from different wheat straw pulps. *Int. J. Biol. Macromol.* **2016**, *92*, 1025−1033.

(10) Liu, D.; Li, Y.; Qian, Y.; Xiao, Y.; Du, S.; Qiu, X. Synergistic Antioxidant Performance of Lignin and Quercetin Mixtures. *ACS Sustainable Chem. Eng.* **2017**, *5*, 8424−8428.

(11) Kai, D.; Low, Z. W.; Liow, S.; Abdul Karim, A.; Ye, H.; Jin, G.; Li, K.; Loh, X. J. Development of Lignin Supramolecular Hydrogels with Mechanically Responsive and Self-Healing Properties. *ACS Sustainable Chem. Eng.* **2015**, *3*, 2160−2169.

(12) Nandiwale, K. Y.; Danby, A. M.; Ramanathan, A.; Chaudhari, R. V.; Subramaniam, B. Zirconium-Incorporated Mesoporous Silicates Show Remarkable Lignin Depolymerization Activity. *ACS Sustainable Chem. Eng.* **2017**, *5*, 7155−7164.

(13) Stewart, D. Lignin as a base material for materials applications: Chemistry, application and economics. *Ind. Crops Prod.* **2008**, *27*, 202−207.

(14) Pucciariello, R.; Bonini, C.; D'Auria, M.; Villani, V.; Giammarino, G.; Gorrasi, G. Polymer blends of steam-explosion lignin and poly($\varepsilon$-caprolactone) by high-energy ball milling. *J. Appl. Polym. Sci.* **2008**, *109*, 309−313.

(15) Dong, X.; Dong, M.; Lu, Y.; Turley, A.; Jin, T.; Wu, C. Antimicrobial and antioxidant activities of lignin from residue of corn stover to ethanol production. *Ind. Crops Prod.* **2011**, *34*, 1629−1634.

(16) Domínguez-Robles, J.; Sánchez, R.; Díaz-Carrasco, P.; Espinosa, E.; García-Domínguez, M. T.; Rodríguez, A. Isolation and character-ization of lignins from wheat straw: Application as binder in lithium batteries. *Int. J. Biol. Macromol.* **2017**, *104*, 909−918.

(17) Azadfar, M.; Gao, A. H.; Bule, M. V.; Chen, S. Structural characterization of lignin: A potential source of antioxidants guaiacol and 4-vinylguaiacol. *Int. J. Biol. Macromol.* **2015**, *75*, 58−66.

(18) Kai, D.; Zhang, K.; Jiang, L.; Wong, H. Z.; Li, Z.; Zhang, Z.; Loh, X. J. Sustainable and Antioxidant Lignin-Polyester Copolymers and Nanofibers for Potential Healthcare Applications. *ACS Sustainable Chem. Eng.* **2017**, *5*, 6016−6025.

(19) Thakur, S.; Govender, P. P.; Mamo, M. A.; Tamulevicius, S.; Mishra, Y. K.; Thakur, V. K. Progress in lignin hydrogels and nanocomposites for water purification: Future perspectives. *Vacuum* **2017**, *146*, 342−355.

(20) Domínguez-Robles, J.; Peresin, M. S.; Tamminen, T.; Rodríguez, A.; Larrañeta, E.; Jääskeläinen, A. S. Lignin-based hydrogels with "super-swelling" capacities for dye removal. *Int. J. Biol. Macromol.* **2018**, *115*, 1249.

(21) Caló, E.; Khutoryanskiy, V. V. Biomedical applications of hydrogels: A review of patents and commercial products. *Eur. Polym. J.* **2015**, *65*, 252−267.

(22) Peppas, N.; Hilt, J.; Khademhosseini, A.; Langer, R. Hydrogels in biology and medicine: From molecular principles to bionanotech-nology. *Adv. Mater.* **2006**, *18*, 1345−1360.

(23) Espinoza-Acosta, J., Torres-Chávez, P., Ramírez-Wong, B., López-Saiz, C., Montaño-Leyva, B. Antioxidant, Antimicrobial, and Antimutagenic Properties of Technical Lignins and Their Applications. *BioResources* **2016**, *11*, DOI: 10.15376/biores.11.2.

(24) Wang, C.; Venditti, R. A. UV Cross-Linkable Lignin Thermoplastic Graft Copolymers. *ACS Sustainable Chem. Eng.* **2015**, *3*, 1839−1845.

(25) Allsopp, A.; Misra, P. The constitution of the cambium, the new wood and the mature sapwood of the common ash, the common elm and the Scotch pine. *Biochem. J.* **1940**, *34*, 1078−1084.

(26) Sarkanen, K. V.; Ludwig, C. H. *Lignins: Occurrence, formation, structure and reactions*; Wiley-Blackwell: New York, 1971; Vol. *10*, DOI: 10.1002/pol.1972.110100315.

(27) García-Domínguez, M. T.; García-Domínguez, J. C.; Feria, M. J.; Gómez-Lozano, D. M.; López, F.; Díaz, M. J. Furfural production from Eucalyptus globulus: Optimizing by using neural fuzzy models. *Chem. Eng. J.* **2013**, *221*, 185−192.

(28) Flory, P. J.; Rehner, J. J. Statistical Mechanics of Cross-Linked Polymer Networks I. Rubberlike Elasticity. *J. Chem. Phys.* **1943**, *11*, 512−520.

(29) Çaykara, T.; Kiper, S.; Demirel, G. Network parameters and volume phase transition behavior of poly(N-isopropylacrylamide) hydrogels. *J. Appl. Polym. Sci.* **2006**, *101*, 1756−1762.

(30) Raj Singh, T. R.; McCarron, P. A.; Woolfson, A. D.; Donnelly, R. F. Investigation of swelling and network parameters of poly-(ethylene glycol)-crosslinked poly(methyl vinyl ether-co-maleic acid) hydrogels. *Eur. Polym. J.* **2009**, *45*, 1239−1249.

(31) Bajpai, S. K.; Singh, S. Analysis of swelling behavior of poly(methacrylamide-co-methacrylic acid) hydrogels and effect of synthesis conditions on water uptake. *React. Funct. Polym.* **2006**, *66*, 431−440.

(32) Ritger, P. L.; Peppas, N. A simple equation for description of solute release I. Fickian and Non-Fickian release from non-swellable devices in the form of slabs, spheres, cylinders or discs. *J. Controlled Release* **1987**, *5*, 23−36.

(33) Costa, P.; Sousa Lobo, J. M. Modeling and comparison of dissolution profiles. *Eur. J. Pharm. Sci.* **2001**, *13*, 123−133.

(34) Larrañeta, E.; Lutton, R. E. M.; Brady, A. J.; Vicente-Pérez, E. M.; Woolfson, A. D.; Thakur, R. R. S.; Donnelly, R. F. Microwave-Assisted Preparation of Hydrogel-Forming Microneedle Arrays for Transdermal Drug Delivery Applications. *Macromol. Mater. Eng.* **2015**, *300*, 586−595.

(35) Donnelly, R. F.; Singh, T. R. R.; Garland, M. J.; Migalska, K.; Majithiya, R.; McCrudden, C. M.; Kole, P. L.; Mahmood, T. M. T.; McCarthy, H. O.; Woolfson, A. D. Hydrogel-Forming Microneedle Arrays for Enhanced Transdermal Drug Delivery. *Adv. Funct. Mater.* **2012**, *22*, 4879−4890.

(36) Larrañeta, E.; Henry, M.; Irwin, N. J.; Trotter, J.; Perminova, A. A.; Donnelly, R. F. Synthesis and characterization of hyaluronic acid hydrogels crosslinked using a solvent-free process for potential biomedical applications. *Carbohydr. Polym.* **2018**, *181*, 1194−1205.

(37) Miles, A. A.; Misra, S. S.; Irwin, J. O. The estimation of the bactericidal power of the blood. *J. Hyg.* **1938**, *38*, 732−749.

(38) Ripolin, A.; Quinn, J.; Larrañeta, E.; Vicente-Perez, E. M.; Barry, J.; Donnelly, R. F. Successful application of large microneedle patches by human volunteers. *Int. J. Pharm.* **2017**, *521*, 92−101.

(39) Donnelly, R. F.; McCrudden, M. T. C.; Zaid Alkilani, A.; Larrañeta, E.; McAlister, E.; Courtenay, A. J.; Kearney, M.; Singh, T. R. R.; McCarthy, H. O.; Kett, V. L.; Caffarel-Salvador, E.; Al-Zahrani, S.; Woolfson, A. D. Hydrogel-Forming Microneedles Prepared from "Super Swelling" Polymers Combined with Lyophilised Wafers for Transdermal Drug Delivery. *PLoS One* **2014**, *9*, No. e111547.

(40) Vinardell, P. M.; Mitjans, M. Lignins and Their Derivatives with Beneficial Effects on Human Health. *Int. J. Mol. Sci.* **2017**, *18*, DOI: 10.3390/ijms18061219.

(41) Ojer, P.; Neutsch, L.; Gabor, F.; Irache, J. M.; López de Cerain, A. Cytotoxicity and cell interaction studies of bioadhesive poly-(anhydride) nanoparticles for oral antigen/drug delivery. *J. Biomed. Nanotechnol.* **2013**, *9*, 1891−1903.

(42) Singh, T. R. R.; McCarron, P. A.; Woolfson, A. D.; Donnelly, R. F. Physicochemical characterization of poly(ethylene glycol) plasticized poly(methyl vinyl ether-co-maleic acid) films. *J. Appl. Polym. Sci.* **2009**, *112*, 2792.

(43) Deepa, A. K.; Dhepe, P. L. Lignin Depolymerization into Aromatic Monomers over Solid Acid Catalysts. *ACS Catal.* **2015**, *5*, 365−379.

(44) Deepa, A. K.; Dhepe, P. L. Solid acid catalyzed depolymerization of lignin into value added aromatic monomers. *RSC Adv.* **2014**, *4*, 12625−12629.

(45) Sclavons, M.; Franquinet, P.; Carlier, V.; Verfaillie, G.; Fallais, I.; Legras, R.; Laurent, M.; Thyrion, F. C. Quantification of the maleic anhydride grafted onto polypropylene by chemical and viscosimetric titrations, and FTIR spectroscopy. *Polymer* **2000**, *41*, 1989−1999.

(46) Donnelly, R. F.; Morrow, D. I.; McCrudden, M. T.; Alkilani, A. Z.; Vicente-Pérez, E. M.; O'Mahony, C.; González-Vázquez, P.; McCarron, P. A.; Woolfson, A. D. Hydrogel-forming and dissolving microneedles for enhanced delivery of photosensitizers and precursors. *Photochem. Photobiol.* **2014**, *90*, 641−647.

(47) Calo, E.; Barros, J. M. S. d.; Fernandez-Gutierrez, M.; San Roman, J.; Ballamy, L.; Khutoryanskiy, V. V. Antimicrobial hydrogels based on autoclaved poly(vinyl alcohol) and poly(methyl vinyl ether-alt-maleic anhydride) mixtures for wound care applications. *RSC Adv.* **2016**, *6*, 55211−55219.

(48) Lutton, R. E. M.; Larrañeta, E.; Kearney, M. C.; Boyd, P.; Woolfson, A. D.; Donnelly, R. F. A novel scalable manufacturing process for the production of hydrogel-forming microneedle arrays. *Int. J. Pharm.* **2015**, *494*, 417−429.

(49) Calo, E.; Barros, J.; Ballamy, L.; Khutoryanskiy, V. V. Poly(vinyl alcohol)-Gantrez® AN cryogels for wound care applications. *RSC Adv.* **2016**, *6*, 105487−105494.

(50) Moreno, E.; Schwartz, J.; Larrañeta, E.; Nguewa, P. A.; Sanmartín, C.; Agüeros, M.; Irache, J. M.; Espuelas, S. Thermosensitive hydrogels of poly(methyl vinyl ether-co-maleic anhydride) - Pluronic(®) F127 copolymers for controlled protein release. *Int. J. Pharm.* **2014**, *459*, 1−9.

(51) Larraneta, E.; Barturen, L.; Ervine, M.; Donnelly, R. F. Hydrogels based on poly(methyl vinyl ether-co-maleic acid) and Tween 85 for sustained delivery of hydrophobic drugs. *Int. J. Pharm.* **2018**, *538*, 147−158.

(52) Capello, C.; Fischer, U.; Hungerbuhler, K. What is a green solvent? A comprehensive framework for the environmental assessment of solvents. *Green Chem.* **2007**, *9*, 927−934.

(53) Larrañeta, E.; Stewart, S.; Ervine, M.; Al-Kasasbeh, R.; Donnelly, R. F. Hydrogels for Hydrophobic Drug Delivery. Classification, Synthesis and Applications. *J. Funct. Biomater.* **2018**, *9*, 13.

(54) Gupta, S. C.; Prasad, S.; Kim, J. H.; Patchva, S.; Webb, L. J.; Priyadarsini, I. K.; Aggarwal, B. B. Multitargeting by curcumin as revealed by molecular interaction studies. *Nat. Prod. Rep.* **2011**, *28*, 1937−1955.

(55) Mohan, P. R. K.; Sreelakshmi, G.; Muraleedharan, C. V.; Joseph, R. Water soluble complexes of curcumin with cyclodextrins: Characterization by FT-Raman spectroscopy. *Vib. Spectrosc.* **2012**, *62*, 77−84.

(56) Weber, D. J.; Anderson, D.; Rutala, W. A. The role of the surface environment in healthcare-associated infections. *Curr. Opin. Infect. Dis.* **2013**, *26*, 338.

(57) Hall, C. W.; Mah, T. F. Molecular mechanisms of biofilm-based antibiotic resistance and tolerance in pathogenic bacteria. *FEMS Microbiol. Rev.* **2017**, *41*, 276−301.

(58) Irwin, N. J.; McCoy, C. P.; Jones, D. S.; Gorman, S. P. Infection-Responsive Drug Delivery from Urinary Biomaterials Controlled by a Novel Kinetic and Thermodynamic Approach. *Pharm. Res.* **2013**, *30*, 857−865.

(59) Shi, H.; Liu, H.; Luan, S.; Shi, D.; Yan, S.; Liu, C.; Li, R. K. Y.; Yin, J. Effect of polyethylene glycol on the antibacterial properties of polyurethane/carbon nanotube electrospun nanofibers. *RSC Adv.* **2016**, *6*, 19238−19244.

(60) Tong, S. Y. C.; Davis, J. S.; Eichenberger, E.; Holland, T. L.; Fowler, V. G. Staphylococcus aureus Infections: Epidemiology, Pathophysiology, Clinical Manifestations, and Management. *Clin. Microbiol. Rev.* **2015**, *28*, 603−661.

(61) Norsworthy, A. N.; Pearson, M. M. From Catheter to Kidney Stone: The Uropathogenic Lifestyle of. *Trends Microbiol.* **2017**, *25*, 304−315.

(62) McKeen, L. W. 3-Plastics Used in Medical Devices. In *Handbook of Polymer Applications in Medicine and Medical Devices*; Modjarrad, K., Ebnesajjad, S., Eds.; William Andrew Publishing: Oxford, 2014; pp 21−53, DOI: 10.1016/B978-0-323-22805-3.00003-7.

(63) Cheng, H.; Li, Y.; Huo, K.; Gao, B.; Xiong, W. Long-lasting in vivo and in vitro antibacterial ability of nanostructured titania coating incorporated with silver nanoparticles. *J. Biomed. Mater. Res., Part A* **2014**, *102*, 3488−3499.

(64) Nudera, W. J.; Fayad, M. I.; Johnson, B. R.; Zhu, M.; Wenckus, C. S.; BeGole, E. A.; Wu, C. D. Antimicrobial Effect of Triclosan and Triclosan with Gantrez on Five Common Endodontic Pathogens. *J. Endod.* **2007**, *33*, 1239−1242.

(65) Boehm, R. D.; Miller, P. R.; Singh, R.; Shah, A.; Stafslien, S.; Daniels, J.; Narayan, R. J. Indirect rapid prototyping of antibacterial acid anhydride copolymer microneedles. *Biofabrication* **2012**, *4*, 011002.

(66) Gabov, K.; Oja, T.; Deguchi, T.; Fallarero, A.; Fardim, P. Preparation, characterization and antimicrobial application of hybrid cellulose-lignin beads. *Cellulose* **2017**, *24*, 641−658.

(67) Yang, W.; Owczarek, J. S.; Fortunati, E.; Kozanecki, M.; Mazzaglia, A.; Balestra, G. M.; Kenny, J. M.; Torre, L.; Puglia, D. Antioxidant and antibacterial lignin nanoparticles in polyvinyl alcohol/chitosan films for active packaging. *Ind. Crops Prod.* **2016**, *94*, 800−811.

(68) Nada, A. M. A.; El-Diwany, A. I.; Elshafei, A. M. Infrared and antimicrobial studies on different lignins. *Acta Biotechnol.* **1989**, *9*, 295−298.

(69) Sun, J.; Wang, W.; Yue, Q. Review on Microwave-Matter Interaction Fundamentals and Efficient Microwave-Associated Heating Strategies. *Materials* **2016**, *9*, 231.